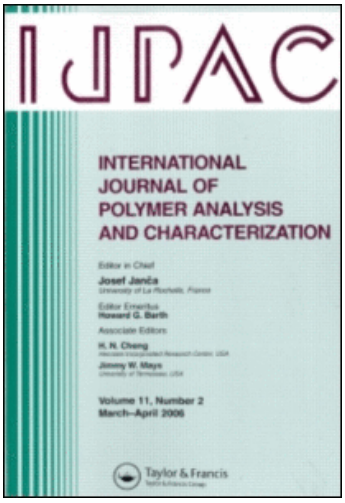

International Journal of Polymer Analysis and Characterization
Publication details, including instructions for authors and subscription information:
http://www.informaworld.com/smpp/title~content=t713646643

Universal Suspension Hydrodynamics: Molecular Characterization of Hydroxypropyl Methylcellulose

Robert Lundqvist[a]
[a] Pharmaceutical and Analytical R&D, AstraZeneca R&D Mölndal, Mölndal, Sweden

To cite this Article Lundqvist, Robert(2005) 'Universal Suspension Hydrodynamics: Molecular Characterization of Hydroxypropyl Methylcellulose', International Journal of Polymer Analysis and Characterization, 10: 5, 259 — 292
To link to this Article: DOI: 10.1080/10236660500479429
URL: http://dx.doi.org/10.1080/10236660500479429

International Journal of Polymer Anal. Charact., 10: 259–292, 2005

ISSN: 1023-666X print
DOI: 10.1080/10236660500479429

Universal Suspension Hydrodynamics: Molecular Characterization of Hydroxypropyl Methylcellulose

Robert Lundqvist
Pharmaceutical and Analytical R&D, AstraZeneca R&D Mölndal, Mölndal, Sweden

Abstract: A study of the rheology of aqueous solutions of hydroxypropyl methylcellulose (HPMC) is presented with the aim of supporting the previously suggested physics, referred to as laminar dynamics, of the viscosity increasing effect per unit volume of particles with extended shape on a flowing suspension. Since it is essential that appropriate flow is employed in order to utilize the proposed model enabling absolute values of the particle's weight average axial ratio $\mathbf{a}_w$ to be derived from the intrinsic viscosity $[\eta]$, the shear requirement is studied extensively. Hence, flow curves (viscosity η versus shear rate) for a series of commercial HPMC viscosity grades (3 to 10,000 cP) of USP substitution type 2910 were measured under an extended range of concentrations c (g/dL) and shear rates D (1/s). The results indicate that $[\eta]$ (dL/g) can be obtained by combining c and D in such a way that either $c \rightarrow 0$ (at constant $D > 0$) or $D > D^*$ (at constant $c > 0$), where D^* is a critical shear rate. It may hence be concluded that laminar dynamics is applicable at any constant $D > 0$ if $c \rightarrow 0$, and it is proposed that such flow corresponds to a complete absence of particle–particle interactions leading to a flow in the vicinity of the particle parallel to its length axis. It is demonstrated that the particle–particle interaction tends to become negligible, i.e., the Huggins constant $k_H \rightarrow 0$ (for extended shape), at any concentration when $D > D^*$. Assuming that the particle–particle interaction is entirely hydrodynamic, i.e., a negligible non-hydrodynamic interaction such as an electrostatic or chemical

The author would like to thank Mr. Lars O. Svensson and Ms. Marie Hedlund for experimental assistance.

Address correspondence to Robert Lundqvist, Pharmaceutical and Analytical R&D, AstraZeneca R&D Mölndal, S-431 83 Mölndal, Sweden. E-mail: robert.lundqvist@astrazeneca.com

interaction, at any D, it is possible to derive a universal suspension hydrodynamics, solely determined by the particle shape and concentration under Newtonian conditions and general to any polymer suspension or solution, by combining stationary dynamics (shown empirically to be a universal relation; $\eta_{sp} = f(c[\eta])$, $D \rightarrow 0$) with laminar dynamics ($\eta_{sp} = c[\eta]$, $D > D^*$ or $c \rightarrow 0$). It is demonstrated how these universal functions can be used for absolute determination of $\mathbf{a}_w$ and subsequent calculation of such values as molecular weight, size, Mark-Houwink constant, critical ("overlap") concentration c^*, and radius of gyration $R_{g,w}$. In addition, a universal suspension characteristic termed critical specific viscosity η^*_{sp} is identified.

Keywords: Hydroxypropyl methylcellulose; Hydrodynamics; Critical shear rate; Critical specific viscosity; Overlap concentration; Polymer

INTRODUCTION

In a preceding article[1] it was shown how it is possible to obtain information about the axial ratio from viscosity measurements of suspensions/solutions of particles with extended shape, e.g., polymers. It was demonstrated that the intrinsic viscosity $[\eta]_\phi$, expressed in terms of dimensionless volume fractions ϕ, simply equals the axial ratio of the particle/polymer if the required conditions for laminar dynamics are met. In order to determine the necessary flow condition, this article concerns the influence of shear rate (i.e., the rheology of the suspension of particles in a liquid). The model polymer used, hydroxypropyl methylcellulose (HPMC), is the same as characterized previously, with osmometry[2] and capillary viscometry,[1] in a broad range of molecular weights M (g/mol), intrinsic viscosities $[\eta]$ (dL/g), and temperatures (°C). In this work the ranges of both shear rate D (1/s) and concentration c (g/dL) are considerably extended.

EXPERIMENTAL SECTION

Materials

Commercial HPMC of USP-substitution type 2910 was obtained from the following manufacturers: Dow Chemical Company (Midland, Michigan, USA) (Methocel E3P and E6P) and Shin-Etsu Chemical Company (Naoetsu, Japan) (Metolose 60SH-6, Metolose 60SH-50, and 60SH-10000). The actual alkoxyl content (% w/w) of the HPMC samples used was $29.0 \pm 0.8\%$ methoxyl and $8.8 \pm 0.8\%$ hydroxypropoxyl, which corresponds to a molar substitution of 1.90 ± 0.05 for the methyl and 0.23 ± 0.03 for the hydroxypropyl groups. Viscosity grades studied were 3 cP, 6 cP, 50 cP, and 10,000 cP. The viscosity grade denotes, following

USP nomenclature, the viscosity (cP or mPas) of a 2% w/v solution at 20°C and low shear rate. Aqueous solutions were prepared by dissolving dried (at 80°C) HPMC samples followed by filtration through a membrane from Millipore (Molsheim, France) (Type AA, 0.8 μm). Solutions having a concentration exceeding about 1 g/dL were not filtered.

Instruments

Couette viscometry was carried out using a Physica Viskolab LC20 (Physica, Messtechnik GmbH, Stuttgart, Germany), equipped with a double-gap measuring system (Z1 DIN54453). The temperature was controlled at 20°C within ±0.1°C with a Lauda RM6 thermostat. Calibration was made with 2000 cP (Type 2000AW, accuracy ±0.4%, Deutscher Kalibrierdienst, Industriepark Wolfen/Thalheim, Germany) and 9 cP (Type Cannon S6, accuracy ±0.25%, Cannon Instrument Company, Pennsylvania, USA) Newtonian viscosity standards.

Measurements

Specific viscosity η_{sp} (dimensionless) was determined as $\eta_{sp} = \eta/\eta^{\circ} - 1$, while intrinsic viscosity $[\eta]$ was obtained by extrapolating the reduced viscosity η_{sp}/c (dL/g) to zero concentration. Here, η (mPas) denotes the viscosity of the suspension/solution and η° its value at zero concentration.[1] A measurement cycle with the Couette apparatus consisted of a run with increased shear rate, from zero to max shear rate, and the reversed run. Since complete reversibility was always observed in these measurements and since four consecutive capillary[1] measurements with the same solution always appeared identical, there was no indication of shear degradation of HPMC under the conditions employed in this work.

THEORY

The general theory of laminar dynamics, i.e., a treatment of the physics of the viscosity increasing effect per unit volume of suspended particles with extended shape in a laminar flow, is outlined in a preceding article.[1] Yet, a few more assumptions (I–III) appear useful.

I. For simplicity, we shall restrict ourselves to the case were the liquid constituent is much smaller than the particle. In this case the axial ratio of the liquid constituents $\mathbf{a}_l$ should have no effect on the viscosity of the suspension, and $\mathbf{a}_l$ may be defined as unity. Hence, the dimensionless intrinsic viscosity $[\eta]_\phi$ obtained by using volume fractions ϕ will approach the weight average axial ratio $\mathbf{a}_w$ of

the particles having extended shape according to Equation (1):

$$[\eta]_\phi = \mathbf{a}_w + 1.5 \cong \mathbf{a}_w \quad (\mathbf{a}_w \gg 1) \tag{1}$$

and where $[\eta]_\phi$ is related to the intrinsic viscosity $[\eta]$ expressed in dL/g through Equation (2):

$$[\eta]_\phi = [\eta]\rho 100 \tag{2}$$

where ρ (g/mL) is a conversion factor (g dry polymer per mL solvated polymer).

II. The flow direction of the liquid in the immediate vicinity of the particle remains parallel to its length axis regardless of Brownian motion.

III. There exists a critical (limiting) shear rate D^* (1/s) above which the distorting effect of the Brownian motion on the orientation of a particle, with a given extended shape, may be considered completely suppressed.

RESULTS AND DISCUSSION

Preliminary investigations indicated that the non-Newtonian behavior of aqueous solutions of HPMC was more pronounced the higher the molecular weight, and therefore emphasis was put on measurements on the highest viscosity grade, i.e., the 10,000 cP grade. However, supplementing information, especially the behavior at high concentration, was gained by measurements on lower viscosity grades: 3 cP, 6 cP, and 50 cP.

Shear Dependence of the Reduced Viscosity

Figure 1 summarizes the results from the Couette viscometry on aqueous solutions of HPMC 10,000 cP. The viscosity has been scaled by transforming it into the logarithm of the reduced viscosity $\log(\eta_{sp}/c)$. The scaling facilitates a mechanistic interpretation as well as a presentation of the greatly varied system, viscosities ranging from 1 to 14,000 cP and concentrations in the range from 0.05 to 2 g/dL. The most important peculiarity of Figure 1, in addition to the shear-thinning behavior, is that the reduced viscosity approaches the intrinsic viscosity $[\eta]$ at any concentration with increasing shear rate. The graph also suggests a common critical rate of shear D^*, approximately 60,000 1/s above which all curves coincide into the same line: $\log(\eta_{sp}/c) = \log[\eta]$. Furthermore, it demonstrates that the extent of non-Newtonian behavior is rapidly decreased with lowered concentration and it indicates that the suspension approaches Newtonian behavior when the concentration approaches zero.

Unfortunately the Couette instrument was not capable of measuring shear rates higher than 4000 1/s, so a direct observation of the suggested

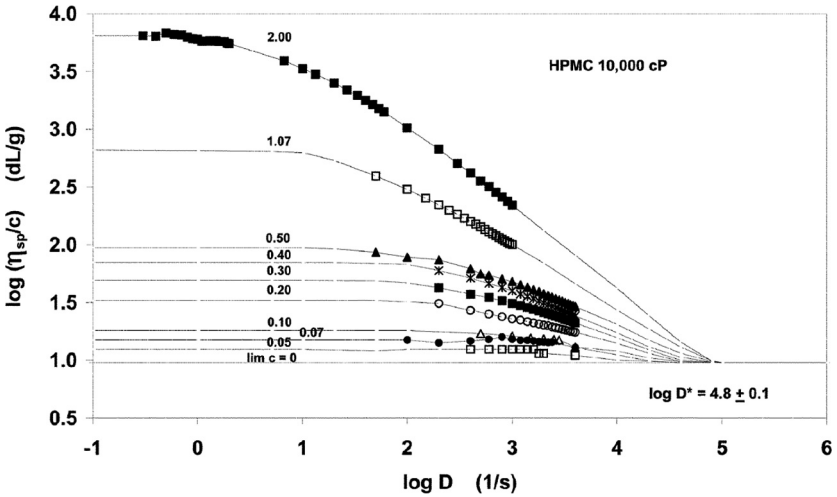

Figure 1. Reduced viscosity log η_{sp}/c (dL/g) as a function of shear rate log D (1/s) for aqueous HPMC 10,000 cP at 20°C and various concentrations c (g/dL). dL). The curves congregate at a critical shear rate log D*.

laminar Newtonian behavior at D > 60,000 1/s was not possible. However, indirect evidence of its existence may be derived by analyzing the concentration dependence at constant shear rate. Figure 2 shows such a plot of log η_{sp} versus log c at constant D. It again indicates that all curves coincide into a single line at sufficiently high shear rate. The slope of this line is unity, and the line can be expressed according to Equation (3):

$$\eta_{sp} = c[\eta] \tag{3}$$

In addition, it can be seen from Figure 2 that Equation (3) becomes valid at any shear rate (D > 0) at sufficiently low concentration, less than about 0.01 g/dL in the case of HPMC 10,000 cP. It also suggests that the intrinsic viscosity $[\eta]$ can be obtained both at any constant shear rate (D > 0) by extrapolating to zero concentration and at any concentration by extrapolation to shear rate = D*. The latter suggestion presumes that aqueous HPMC is equally extended at any shear rate.

Shear Dependence of the Huggins Interaction Constant

The concentration dependence of the reduced viscosity is frequently expressed as a truncated polynomial expression according to Equation (4):

$$\eta_{sp}/c = [\eta] + k_H[\eta]^2 c + \cdots \tag{4}$$

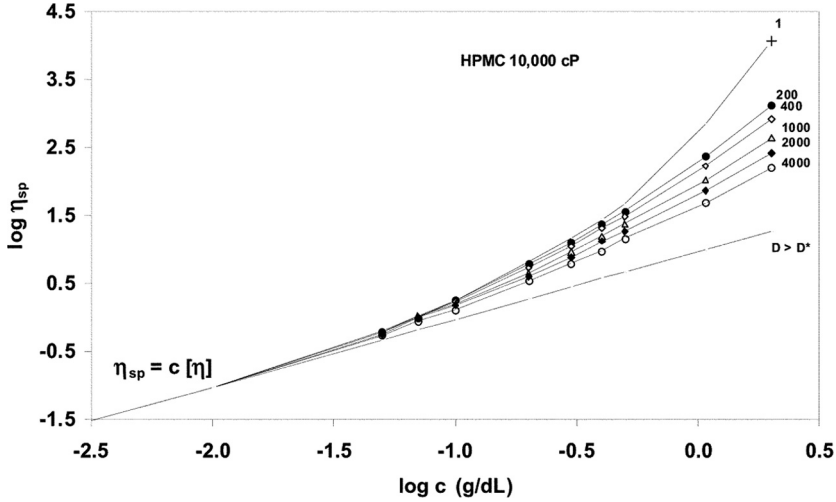

Figure 2. Specific viscosity log η_{sp} as a function of concentration log c (g/dL) for aqueous HPMC 10,000 cP at 20°C and various constant shear rates D (1/s). The lines converge to a single line, $\eta_{sp} = c[\eta]$, at sufficiently low concentration or high shear rate.

where k_H, usually referred to as the Huggins constant or the interaction constant,[3] may be viewed as generally reflecting the combined hydrodynamic and chemical interaction.[1] However, under laminar Newtonian conditions, k_H appears to be entirely due to hydrodynamic interactions, as was concluded before,[1] to account for the fact that k_H was unaffected by an appreciable chemical variation (brought about by decreasing the hydration with an increase in temperature).[1]

Figure 3 presents the observed concentration dependence of η_{sp}/c at constant shear rates ranging from 200 to 4000 1/s for HPMC 10,000 cP. Curves for very low shear rate (D = 1 1/s) and very high shear rate (D = 100,000 1/s) have been obtained by extrapolating data from Figures 1 and 2. It is evident that the linearity of the concentration dependence of the reduced viscosity is restricted to concentrations lower than a certain concentration c_{lin}, which approximately equals the frequently used[4] "overlap" concentration c^*. Furthermore, it appears as if these approximate c^* values approach a finite value as the shear rate approaches zero, while they steadily increase with increased shear rate approaching unit volume fraction (i.e., $c^* \to 100\rho$ g/dL) at infinite D. The values of c_{lin} and k_H for aqueous HPMC are collected in Tables I and II, which show that k_H approaches a finite value of about 0.6 ± 0.2 (dimensionless) as D→0, while k_H becomes zero at sufficiently large D ($D > D^*$, see Figures 2 and 3). The results are consistent with

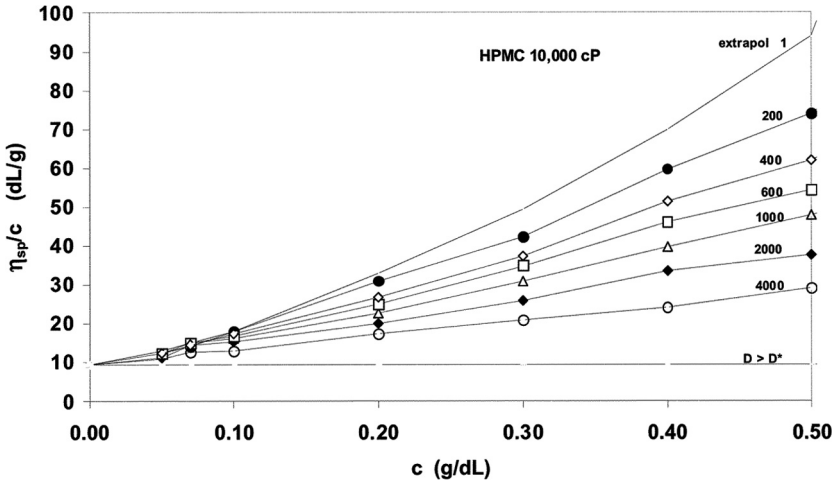

Figure 3. Linear plot of reduced viscosity η_{sp}/c vs. concentration c (g/dL) for aqueous HPMC 10,000 cP at 20°C and various constant shear rates D (1/s). The decreasing slopes with increasing D indicate that Huggins constant $k_H \to 0$ as $D \geq D^*$. Likewise, a limiting value of k_H is indicated as $D \to 0$.

the view that k_H reflects hydrodynamic interactions only at conditions where the particle–particle interaction is negligible, i.e., at sufficiently low concentration or at sufficiently high shear rate.

General Shape of the Flow Curves

The above findings can be used to construct complete flow curves for the HPMC solutions. Hence, all experimental and theoretical information

Table I. Linear range concentrations c_{lin} and Huggins interaction constants k_H for aqueous HPMC 10,000 cP determined with Equation (4) from data in Figure 3 at constant shear rate D using Couette viscometry at 20°C

Shear rate range (1/s)	c_{lin} (g/dL)	k_H dimensionless
1	0.07 ± 0.03	0.8 ± 0.2
1,000	0.12 ± 0.05	0.7 ± 0.1
2,000	0.5 ± 0.1	0.6 ± 0.1
4,000	>0.5	0.4 ± 0.1
100,000	>0.2	0
∞	96 est[a]	0

[a] $c_{lin} \approx c^* = 100/\rho$, where $\rho = 1.04$ g (dry polymer/mL solvated polymer) is a conversion factor to volume fraction.[1]

Table II. Linear concentration ranges c_{lin}, "overlap" concentrations c^*, and Huggins interaction constants k_H at stationary conditions (D→0 1/s) for aqueous HPMC of various viscosity grades estimated with Couette viscometry at 20°C

HPMC Viscosity grade 2% w/v, 20°C cP	$[\eta]$ 20°C,[a] dL/g	Linear conc. range, c_{lin} 20°C g/dL	k_H 20°C unit less	c^* Equation (24) g/dL
10,000	9.58 ± 0.12	$0.07 + 0.03$	0.8 ± 0.2	0.13
50	2.67 ± 0.05	0.7 ± 0.2	0.6 ± 0.1	0.47
6	0.91 ± 0.03	1.4 ± 0.3	0.7 ± 0.2	1.38
3	0.69 ± 0.02	1.8 ± 0.3	0.6 ± 0.1	1.83

[a]Capillary viscometry.[1]

may be combined as shown in Figure 4, which depicts the flow curves in terms of the relations between shear force τ (mPa) and shear rate D (1/s) in a log-log plot for various concentrations. The curves have a typical sigmoid shape showing two Newtonian regions characterized by parallel lines having unit slope. The separation between the two lines decreases with decreased concentration so that they coincide into one single line as the concentration approaches zero. The two Newtonian regions at low and high shear rates may be termed stationary Newtonian and high-shear Newtonian, respectively. Stationary Newtonian conditions

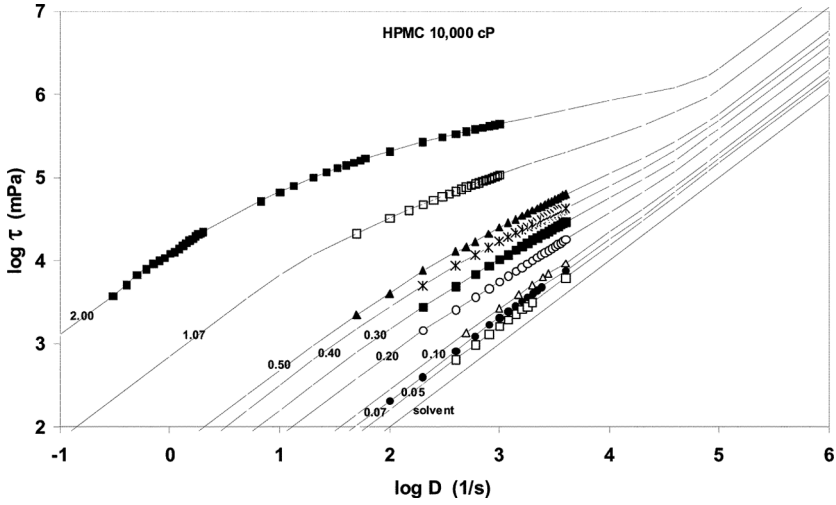

Figure 4. Flow curves, $\log \tau$ (mPas) vs. $\log D$ (1/s), for aqueous HPMC 10,000 cP at 20°C and various concentrations c (g/dL). Extrapolations are made according to theory.

thus occur at near-zero shear rate while high-shear Newtonian conditions occur above a critical shear rate D^* characteristic of the particle shape (D^* is about 60,000 1/s for HPMC 10,000 cP). According to laminar dynamics (see Equation (3)), the high-shear Newtonian region corresponds to shear independent reduced viscosity equal to the intrinsic viscosity.

The sigmoid shape and the existence of two Newtonian regions for shear-thinning suspensions/solutions are generally recognized rheological behavior[5–15] in accordance with the pioneering work on colloids (''Ostwald-curves'' demonstrating only the high-shear Newtonian region)[16] and polymer solutions by Reiner (first general flow curve ''Konsistenzkurve'' recognizing also the low-shear Newtonian region) and by Philippoff and coworkers and later work by Timell, Merrill, and Yang on rubber,[17,18] celluloses,[19–22] polyisobutylene,[23,24] polystyrene,[25] and polypeptides.[26,27] The rheology of the shear-thinning region between the two Newtonian regions corresponds to the behavior of ''power-law'' fluids or ''Ostwald-de Waele'' fluids since the central part of this region shows linear relations between log η and log D with slopes between 0 and -1.[5,6,8,9,11–14,28–30]

Philippoff and coworkers[22] and Merrill[24] found, in agreement with the present work, that η_{sp}/c becomes constant independent of concentration, equaling $[\eta]$ at sufficiently high shear rate. However, in their earlier work and also in the work of Yang[26,27] values of η_{sp}/c even lower than $[\eta]$ were occasionally indicated. The reason for these latter observations may be that the systems studied did not obey all of the necessary conditions for obtaining laminar dynamics. In fact, the rheological conditions of these systems were extreme as a result of a combination of high shear rate (up to 10^6 1/s) and high $[\eta]$ (up to 46 dL/g).[19] Possibly, too high shear stress might have led to a slippage (shearing or friction) between the particle and liquid leading to violation of the adherence requirement.[1] Another possibility is experimental difficulties due to viscous heat generation.[31] Nevertheless, at high frequencies of alternating shear stress, a few systems that behave just opposite to the above systems in that the high frequency $[\eta']$, where η' is the dynamic viscocity, is independent of shape (molecular weight and branching) and dependent only on polymer chemistry have been reported by Ferry.[10] These systems, studied with oscillatory viscometry, appear to represent another hydrodynamic case, possibly dominated by the above-mentioned slipping, but which is not the issue of this work.

Surprisingly, although obvious from the experimental results in the above-cited polymer literature, it was not explicitly stated that k_H is shear dependent and that k_H actually approaches zero at sufficiently high shear rate. However, using other theoretical arguments, Berry and Russel[32] propose that k_H for rods decreases to zero with increasing Peclet number,

which is further supported by observations of Chauveteau[33] on high molecular weight xanthan in 0.1 M NaCl, although the additional effect of slipping is also indicated at high shear stress as a decrease in apparent [η].

Recently, Tsenoglou[34] has, in line with the present work, assumed that the shear-thinning ceases at a characteristic high shear rate. However, neither the suggested independence of molecular weight of this characteristic shear rate nor the influence of the molecular weight on the slope of the flow curve are in accordance with the experimental observations reported here.

Rheology of Low Viscosity Grade HPMC

Figure 5 shows the shear rate dependence of the reduced viscosity for the 50 cP grade in a way similar to that for the 10,000 cP grade presented in Figure 2. It is obvious that the shear-thinning sensitivity of the polymer decreases rapidly with decreased viscosity grade. The effect is perhaps more striking in terms of axial ratio $\mathbf{a}_w$ or [η], which both are changed by a factor of approximately 3.6 (for intrinsic viscosity [η] see Table II). If taking the critical shear rate D^* as a measure of the shear-thinning sensitivity, a comparison of Figures 1 and 5 shows that this must decrease approximately one decade from 10,000 to 50 cP since D^* appears to increase from about 60,000 to about 800,000. It can also be inferred from

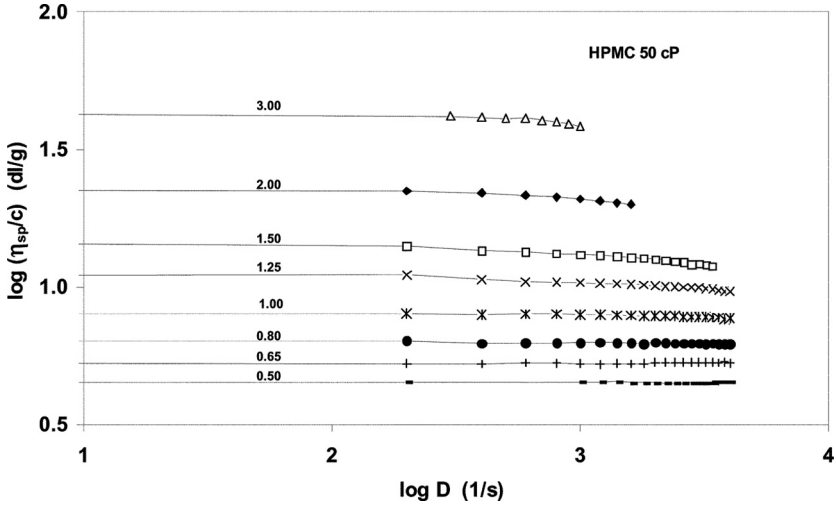

Figure 5. Flow curves, log η_{sp}/c (dL/g) vs. log D (1/s), for aqueous HPMC 50 cP at 20°C and various concentrations c (g/dL). The curves demonstrate a weak shear-thinning effect for c > 0.8 g/dL and D > 4000 1/s.

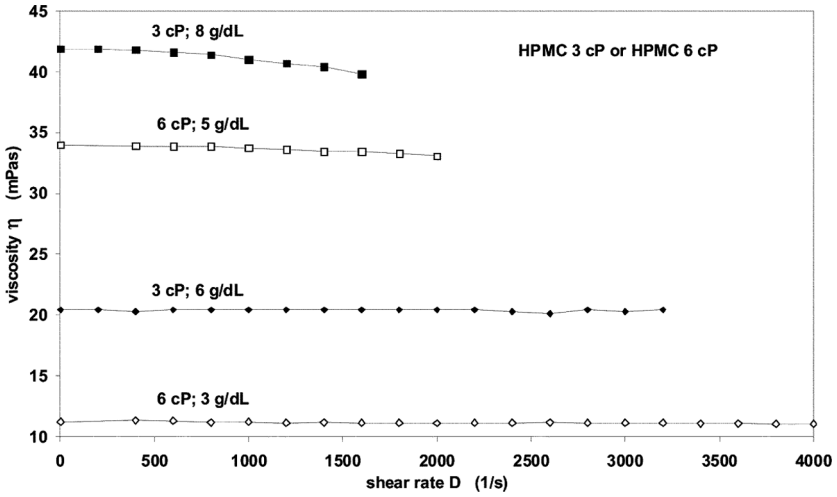

Figure 6. Flow curves, η (mPas) vs. D (1/s), for aqueous HPMC 3 cP and HPMC 6 cP at 20°C and various concentrations c (g/dL). The curves demonstrate a weak shear-thinning effect only at high concentrations (>3 g/dL and >4000 1/s for 6 cP and >6 g/dL and >3200 1/s for 3 cP).

Figure 5 that shear thinning for the 50 cP Grade HPMC is not detectable for <0.8 g/dL concentration at shear rates <4000 s^{-1}. The general trend of decreased shear thinning with decreased viscosity grade continues for the 6 cP and 3 cP grades as shown in Figure 6. Here it can be seen that shear thinning is not detectable for <3 g/dL at <4000 s^{-1} and for <6 g/dL at <3200 s^{-1} for 6 cP and 3 cP, respectively.

Universal Suspension Hydrodynamics

Stationary Conditions (D→0)

If the conclusion reached earlier[1] that the Huggins constant is entirely due to hydrodynamic interactions in the case of sufficiently dilute particle dispersions (polymer solutions) is assumed to extend to higher concentrations where the reduced viscosity is no longer linear against the concentration but exponentially increasing, one should be able to bring particles of any axial ratio **a** into a universal function $\eta_{sp} = f(\mathbf{a},c)$. One way to accomplish this is to rewrite Equation (4) into Equation (5):

$$\eta_{sp} = k_1(c[\eta])^1 + k_2(c[\eta])^2 + \cdots + k_j(c[\eta])^j \cdots \quad (5)$$

where $k_1 = 1$, $k_2 = k_H$, and all k_j are independent of $[\eta]$.

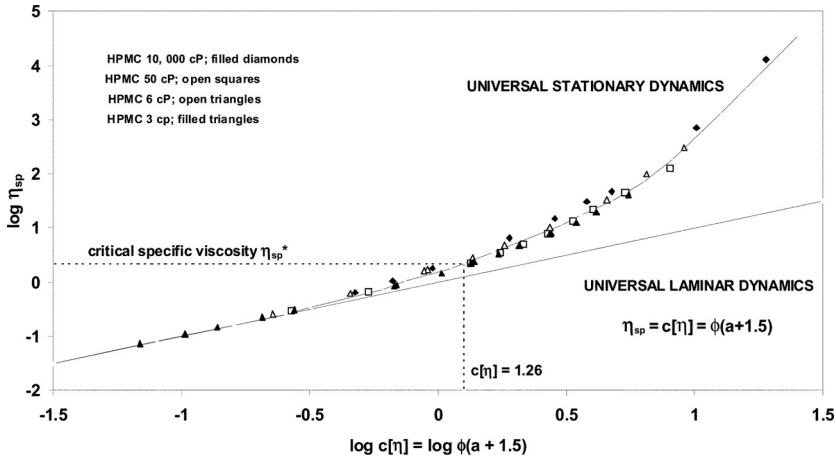

Figure 7. Universal dynamics, $\log \eta_{sp}$ vs. $\log c[\eta] = \log \phi(\mathbf{a}_w + 1.5)$, for aqueous HPMC of various viscosity grades (3 cP to 10,000 cP) and concentrations (0.05 g/dL to 10 g/dL) at 20°C and stationary conditions (D→0 1/s). The line with slope 1 corresponds to universal laminar dynamics; $\eta_{sp} = c[\eta] = \phi(\mathbf{a}_w + 1.5)$. Also shown is the universal critical specific viscosity η_{sp}^* ($\eta_{sp}^* \approx 2.2$) corresponding to slope 1 of $\log \eta_{rel}$ vs. $\log c[\eta]$.

Figure 7 shows the result of scaling according to Equation (5) by plotting $\log \eta_{sp}$ versus $\log(c[\eta])$ at stationary Newtonian conditions (i.e., D→0) for aqueous HPMC. The coalescence of the data for all viscosity grades, ranging from 3 to 10,000 cP (see Table II), into a single curve, $\eta_{sp} = f(c[\eta])$ supports the above assumption of a universal behavior.

Empirically, a universal function for the concentration dependency of the relative viscosity, $\eta_{rel} = \eta_{sp} + 1$, according to Equation (6):

$$\eta_{rel} = \left(\frac{1 + c[\eta]}{k}\right)^k \tag{6}$$

was found long ago by Baker,[35] who used k = 6 to k = 7 in the equivalent notation $\eta_{rel} = (1 + ac)^k$, where ak can be shown to correspond to $[\eta]$, and which equation was later used by Philippoff[19,20] (who used k = 8) to accurately describe the concentration dependency for various types of polymers up to high η_{rel} (at least $\eta_{rel} = 10^5$). Equation (6) is attractively simple, having only one adjustable parameter k, and appears to be remarkably useful as a numerical tool, being accurate and of correct form when c→0 and apparently providing reasonable accuracy up to very high concentrations (if $\mathbf{a} \gg 1$). The broken curve in Figure 7 has been obtained by using k = 7.2, which fits all the experimental results for aqueous HPMC, from $\eta_{sp} = 0$ to $\eta_{sp} = 10^5$.

There is other literature support for the universal behavior by Onogi et al.,[36,37] Johnson et al.,[38] and Takada et al.[39] Onogi et al. found that "master curves" $\log \eta$ versus $\log c$ or $\log M$ can be obtained for polystyrene and polyvinylacetate in a given solvent and at constant temperature by shifting the curves along the $\log c$ or $\log M$ axis. Johnson et al. concluded that polyisobutylene of various molecular weights in the investigated concentration range, up to about 18 g/dL, in both xylene and decalin at 25°C superimpose in a graph log η_{rel} versus log(c $M^{0.68}$). Takada et al. showed that widely varied aqueous xantane solutions ([η] from 0.7 to 71 dL/g and concentrations from 0.005 to 9 g/dL) containing 0.1 M NaCl at 25°C can be scaled using c[η]. In fact, the data give fair agreement with Equation (6) in the entire investigated range; from $\log \eta_{sp} = -0.9$ to $\log \eta_{sp} = 6.3$. Interestingly enough, Ohshima et al.'s[40,41] viscosity data for greatly varied poly-hexylisocyanate solutions ([η] from 0.2 to 85 dL/g g in dichloromethane at 20°C,[40] toluene at 25°C,[41] and hexane at 40°C[41]) appear to deviate from the universal behavior at high c[η]. Lower η_{sp} values than expected from Equation (6) are found for c[η] > 7, corresponding to $\log \eta_{sp} > 2$, indicating that the fundamental requirements of laminar dynamics are not obeyed, or that **a** is decreasing, at high c[η]. Possibly, an onset of molecular aggregation or folding may account for this. In any case, the highest concentrations approached the point where formation of a nematic phase started.

The dimensionless product c[η] can be substituted for $\phi[\eta]_\phi$ or $\phi(\mathbf{a}_w + 1.5)$, since $c[\eta] = \phi[\eta]_\phi = \phi(\mathbf{a}_w + 1.5)$, where ϕ is the volume fraction of particles.[1] This substitution is advantageous since **a** is physically more correct and may vary with the system composition while [η] is restricted to infinite dilution. Consequently, both the weight average axial ratio $\mathbf{a}_w$ and [η] for any particle or polymer can be obtained from any of the universal functions, either in the form $\log \eta_{sp}$ versus $\log(\phi(\mathbf{a}_w + 1.5))$ or in the form $\log \eta_{sp}$ versus log(c[η]), as exemplified by Equations (5) and (6), and Figure 7.

Laminar Conditions ($D > D^*$ or $c \rightarrow 0$)

The conditions of laminar dynamics can be expressed as $\eta_{sp} = c[\eta]$, at any c, provided D is sufficiently large. Since the same expression for η_{sp} is obtained as a limiting case when $c \rightarrow 0$, from stationary dynamics it is evident that both these Newtonian dynamics become indistinguishable at sufficiently large dilution; see Figure 7.

Shear-Thinning Conditions ($D < D^*$ and $c > 0$)

Although both stationary and laminar dynamics are shown to be solely dependent upon particle shape and concentration, it can be anticipated

that the shear-thinning behavior will be more complicated (see the sections on the influence of Brownian motion and critical shear rate D^* below). However, if the temperature is kept constant for a given polymer it should be possible to obtain some information about the effect of shape also at shear-thinning conditions. Furthermore, if the orientation of the particles is assumed to be unaffected by the concentration one should be able to isolate the effect of **a** by studying the flow curve, log η_{sp} versus log D, at constant c[η]. This would result in the same η_{sp} at both stationary Newtonian and laminar Newtonian conditions. An example of such an analysis is given in Figure 8 under ''iso-Newtonian'' conditions at c[η] = 3.9 ± 0.1 (dimensionless) utilizing a pair of aqueous HPMC solutions (1.5 g/dL 50 cP and 0.4 g/dL 10,000 cP). The two solution have practically the same η_{sp} at stationary and high-shear conditions, and the flow curves are shifted parallel to the D axis. The shift indicates that D^* is inversely proportional to the square of **a** for a fully extended polymer.

In the literature it has been noted that the low shear range of the shear-thinning region demonstrates evidence of universality.[15,42–44] Such low shear flow curves can often be normalized into a single master curve, $\eta/\eta_0 = f(D\lambda)$, where η_0 is the viscosity at zero shear rate and λ a chosen characteristic time constant for each condition (different molecular

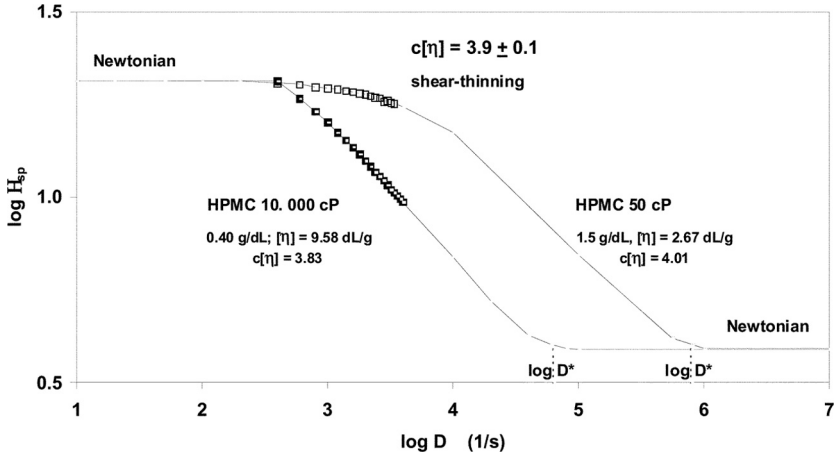

Figure 8. Flow curves, log η_{sp} vs. log D (1/s), at ''iso-Newtonian'' conditions for a pair of aqueous HPMC solutions at 20°C and at constant c[η]; 1.5 g/dL HPMC 50 cP and 0.40 g/dL HPMC 10,000 c, both having c[η] = 3.9 ± 0.1 (dimensionless). Extrapolations are made according to theory that indicates that the curves coincide at the two Newtonian regions occurring at low and high D. The splitting of the curves in the intermediate shear-thinning region is characterized by their different critical shear rates D^*.

weights, concentrations, temperatures, and chemical species).[44] Generally, a master curve, $\eta_{sp}/\eta_{sp0} = f(D\lambda)$, appears to be constructable provided that η is sufficiently large compared to its value η_∞ in the high-shear Newtonian range (i.e., at $D \geq D^*$). Such a master flow curve was created from combined literature (polystyrene in toluene[42] and polyacrylamide in water[45]) and the present HPMC data and was found to support the power law extrapolations made in Figures 1, 2, and 8. However, construction of a complete flow curve, including both Newtonian ranges, requires additional parameters[7,9,11] (η_∞ and at least one adjustable parameter m as in the equation $\eta = \eta_\infty + (\eta_0 - \eta_\infty)/[1 + (D\lambda)^m]$ suggested by Cross[7]). Since laminar dynamics allows η_∞ and η_0 to be estimated, from Equation (3) ($\eta_\infty/\eta^\circ = c[\eta] + 1$) and Equation (6), the entire flow curve can be described using only the two adjustable constants λ and m.

CONCLUSION

Universal Suspension Hydrodynamics

Defining suspension hydrodynamics as the physics of the effect of various variables on the specific viscosity per unit volume of suspended particles (i.e., on the reduced specific viscosity η_{sp}/ϕ) it has been demonstrated (above and previously[1]) that the hydrodynamics under Newtonian conditions, as described by the proposed stationary and laminar dynamics, is universal in the sense that it is identical for any particle (or polymer) or solvent at any temperature provided that the model requirements are fulfilled. These can be summarized as: (1) negligible particle–particle interaction, (2) large particles, in comparison with the liquid constituents, and (3) axial ratio $\mathbf{a} >> 1$. These requirements put limits on the validity of the suggested universal functions; see Equations (3) and (5).

Concentration Limits

The highest particle concentration possible should be determined by the point where the liquid is no longer the continuous and unordered phase. This means that bulk particle systems (e.g., polymer melts) are theoretically exempted while high concentrations approaching unit volume fraction might still be valid, especially if the particles are uncharged. Concentrations in this study were up to only 10 g/dL but the literature gives examples of systems that appear to comply with the stationary dynamics for as high as 50 g/dL (e.g., up to 47 g/dL polystyrene in toluene at 40°C,[36] up to 55 g/dL polystyrene in n-butylbenzene at 30°C,[42,46] and up to 36.5 g/dL for cellulose acetate in acetone or cyclohexanone at 25°C[19,20,47]).

Size Limits

No exact value of the relative size V_p/V_l, where V_p = volume of particle and V_l = volume of the liquid constituents (solvent molecules), can be given. However, it appears from literature[48] data that a value of 5 is not sufficient since the concentration dependence, up to 40 g/dL, for squalene in benzene (V_p/V_l approximately 5) seems to be much weaker than expected from stationary dynamics. For still lower values the concentration dependence might even be negative, see Part II, giving rise to negative $[\eta]$.

Axial Ratio Limits

Although $\mathbf{a} >> 1$ is theoretically required, axial ratios approaching unity, i.e. spheres, give close agreement with stationary dynamics up to surprisingly high concentrations. Appreciable deviation occurs only at concentrations above about 10 g/dL, as can be inferred from viscosity data on aqueous sucrose at 20°C.[49] However, one notes that the viscosity increasing effect, per unit volume and axial ratio ($\phi\mathbf{a}$), is stronger for spheres than for extended shape particles, very slightly at low concentrations but progressively stronger at higher concentration. The phenomenon is consistent with the theory of laminar dynamics.

Molecular Characterization

Although only particle shape $\mathbf{a}_w$ is directly measurable from the universal suspension hydrodynamics, it is possible, using supplementary molecular information of, for example, the exponent α of the Mark-Houwink equation $[\eta] = KM^{\alpha}$, the molecular weight M, or the radius of gyration R_g, to obtain additional information about the polymer using the following relations derived from laminar dynamics.[1] In order to facilitate numerical and graphical analysis over the entire range of degree of polymerization DP, appropriate relations for the theoretical rod-shaped monomer unit are also given.

Molecular Weight

Employing the chain-folding hypothesis,[1] i.e., that flexible polymers may fold 180° to form dense rod-shaped unflexible particles, and where α is a measure of the resistence to fold, one may calculate the weight average M_w from Equation (7):

$$M_w = \left(\frac{\mathbf{a}_w}{\mathbf{a}_u}\right)^{1/\alpha} M_u \tag{7}$$

where $\mathbf{a}_w = [\eta]\ 100\rho$, $\mathbf{a}_u$ is the axial ratio of the monomer unit including solvation, and M_u is the molecular weight (g/mol) of the monomer unit. It follows that the weight average DP_w equals $(\mathbf{a}_w/\mathbf{a}_u)^{1/\alpha}$.

Mark-Houwink Constant K_w

Weight average K_w (dL/g(g/mol)$^{-\alpha}$) can be obtained using Equation (8):

$$K_w = \frac{\mathbf{a}_u (M_u)^{-\alpha}}{(100\rho)} \tag{8}$$

In terms of DP the constant K_{DPw} (dL/g) becomes dimensionally simpler: $K_{DPw} = \mathbf{a}_u/(100\ \rho)$ and the Mark-Houwink equation can be written as

$$[\eta] = \frac{\mathbf{a}_u DP_w^{\alpha}}{(100\rho)} \tag{9}$$

from which it can be concluded that any polymer suspension (solution) having the same α and DP will both have practically the same $[\eta]$ and viscosity concentration profile (see Equation (6)), varying only slightly according to the characteristic value $\mathbf{a}_u/\rho$ (mL/g). The corresponding number average constants are obtained using the relations $K_n/K_w = K_{DPn}/K_{DPw} = P^{\alpha}$, where P is the polydispersity ($P = M_w/M_n$). Equation (8) is supported by the observation that K_w and α are functions of each other; $\log K_w = C - B\alpha$, where C and B are characteristic constants for a given polymer.[50]

Intrinsic Viscosity of the Repeating Unit

The weight and number average intrinsic viscosities of the rod-shaped monomer unit are defined according to Equation (10):

$$[\eta]_{u,w} = \frac{\mathbf{a}_u}{(100\rho)} = [\eta]_{u,n} P^{-\alpha} \tag{10}$$

Size

The dimensions of the rod-shaped molecule can be estimated assuming it to consist of a folded polymer chain with ψ strands with diameter $d_u = l_u/\mathbf{a}_u$ (where d_u and l_u are the diameter and length of the repeating unit) so that the particle diameter becomes $d = d_u \psi^{1/2}$. The weight averages of the number of strands ψ_w, length l_w (cm), and diameter d_w (cm) can then be resolved[51] from Equations (11), (12), and (13):

$$\psi_w^{3/2} = \frac{M_w\, \mathbf{a}_u}{(M_u \mathbf{a}_w)} = DP_w^{(1-\alpha)} \tag{11}$$

$$l_w^3 = \frac{l_u^3 M_w \mathbf{a}_w^2}{(M_u \mathbf{a}_u^2)} = l_u^3 DP_w^{(1+2\alpha)} \tag{12}$$

$$d_w^3 = \frac{l_u^3 M_w}{(M_u \mathbf{a}_w \mathbf{a}_u^2)} = \frac{l_u^3 DP_w^{(1-\alpha)}}{\mathbf{a}_u^3} \tag{13}$$

where l_u is in cm. If fully extended (i.e., $\alpha = 1$) Equations (12) and (13) give $\mathbf{a}_w = l_u DP_w/d_u = \mathbf{a}_u DP_w$ in agreement with Flory.[52] The weight average polymer contour length L_w (i.e., the chain length) is defined as $L_w = DP_w l_u$.

Axial Ratio of the Repeating Unit

The value of $\mathbf{a}_u$ can be derived from the volume, length, and cross-sectional form of the rod-shaped monomer unit. In case the cross section is circular a value of $\mathbf{a}_u$, including solvation, can be estimated from l_u, determined, for example, by crystallography, according to Equation (14):

$$\mathbf{a}_u^2 = \frac{\rho N_A \pi l_u^3}{(4M_u)} \tag{14}$$

where N_A is the Avogadro number (number/mol).

Radius of Gyration $R_{g,w}$

Treating all polymers as being essentially rod shaped, irrespective of degree of extension or α, according to the above folding assumption, one may estimate the weight average $R_{g,w}$(cm) from the definition of radius of gyration R_g; R_g^2 is the weight average squared distance to the center of mass.[53] One arrives at Equation (15):[53]

$$R_{g,w} = \frac{l_w}{(12)^{1/2}} = \frac{l_w}{3.46} \tag{15}$$

Insertion of Equations (12) and (7) gives

$$R_{g,w} = \frac{l_u DP_w^{(1+2\alpha)/3}}{(12)^{1/2}} \tag{16}$$

from which it follows that $R_{g,w}$ should be proportional to $DP_w^{(1+2\alpha)/3}$.

Radius of Gyration of the Repeating Unit

In accordance with the above, the radius of gyration for the rod-shaped monomer unit will be defined by

$$R_{g,u,w} = \frac{l_u}{(12)^{1/2}} = \frac{l_u}{3.46} \tag{17}$$

Flory Radius of the Hydrodynamic-Equivalent Sphere R_F

The conventional Flory radius R_F of an expanded coil, as if carrying associated solvent,[54] with spherical shape can be calculated from its definition:

$$R_F^3 = \frac{100\,[\eta]\,M_w\,3}{(2.5\,N_A\,4\pi)} \tag{18}$$

Insertion of Equation (7) and $[\eta] = \mathbf{a}_w/(100\rho)$ yields

$$R_F^3 = \frac{M_w^{(1+\alpha)}\,3\,\mathbf{a}_u}{(2.5 N_A 4\,\pi\,\rho\,M_u^{\alpha})} \tag{19}$$

from which it is seen that R_F is proportional to $M_w^{(1+\alpha)/3}$.

Radius of Gyration of the Flory Sphere $R_{g,F}$

Generally, the density of repeating units for an expanded coil diminishes with increased distance r from the mass center according to various models.[53,55] In the case of the Flory sphere the density must be proportional to $r^{-(3-3/(1+\alpha))}$ in order to comply with Equation (19) and the radius of gyration can therefore be derived exactly:

$$R_{g,F}^2 = \frac{3}{(5+2\alpha)R_F^2} \tag{20}$$

The value of $R_{g,F}$ will thus depend slightly on α, and the highest α is expected for a fully expanded chain which for a Flory coil is equivalent to a rod with length $2R_F$. Such extension is also equivalent to a coil with a density of repeating units proportional to r^{-2}, which requires $\alpha = 2$, resulting in $R_{g,F} = 0.577R_F$ ($\alpha = 2$) and which result independently is obtained from Equation (15) for $l_w = 2R_F$. It is of interest that the same conclusion, i.e., that the expanded hydrodynamic volume concept requires $\alpha = 2$ for rods, was reached already at the introduction of the concept using other arguments.[56–61] However, full extension does not correspond to $\alpha = 2$ but to $\alpha = 1$ as postulated by laminar dynamics and supported by experimental Mark-Houwink relations for rigid rods. Hence, the expanded hydrodynamic volume concept does appear to reflect a virtual rather than real phenomenon.[1] Full extension, according to Laminar dynamics, corresponds to $R_{g,F} = 0.654R_F$ ($\alpha = 1$). Incomplete extension may be exemplified with $R_{g,F} = 0.707R_F$ ($\alpha = 0.5$) and $R_{g,F} = 0.775R_F$ ($\alpha = 0$). The latter case is identical to the result for the dense sphere.[53]

Radius of gyration of a dense sphere $R_{g,s}$.

Since the radius of gyration for a dense sphere $R_{g,s}$ is equal to $(3/5)^{1/2} = 0.775$ times the physical radius of the sphere[53] one obtains

$$R_{g,s}^3 = \frac{(3/5)^{3/2} 3 M_w}{(\rho N_A 4\pi)} \quad (21)$$

Ranking of Radii

According to the above analysis one can, in the case $M_w \gg M_u$ and $\alpha \leq 1$, arrange the various radii after increased size as follows:

$$R_{g,s} < R_{g,F} < R_F < R_{g,w} \quad (22)$$

Molecular Characteristics of HPMC

Table III summarizes the calculated values of $M_w, l_w, R_{g,w}, R_F, R_{g,F}$, and $R_{g,s}$ for the various viscosity grades of HPMC using the measured $[\eta]$ and the following constants: ρ, M_u, l_u, and $\alpha = 1$. The M_w values are larger than previously calculated,[1] due to a new estimate of $\mathbf{a}_u$ ($\mathbf{a}_u = 0.58 \pm 0.04$) from the crystallographic length ($l_u = 5.15$ Å) of the repeating glucose unit in cellulose,[62] according to Equation (14). The grade average M_w values agree well with single batch values measured with static light scattering (FFF-MALS).[63] However, experimental values of $R_{g,z}$ for HPMC are both meager[63–66] and subject to considerable variation, preventing a conclusive comparison with the calculated values. Hence, $R_{g,z}$ values for some other celluloses, all of which should have the same length of the repeating main chain glucose unit (aqueous xanthan[67], hydroxyethyl cellulose, HEC,[68] and nonaqueous cellulose acetate, CA[69]), with comparable DP_w have been included in Table III. Despite the experimental uncertainty in the measured $R_{g,z}$ values these indicate that HPMC is highly extended and that the proposed rod shape is at least as realistic as the spherical shape (dense sphere or the expanded Flory hydrodynamic-equivalent sphere). The calculated radii of gyration appears to be in good agreement with the measured values, especially for xanthan, as long as the molecule dissymmetry is not too high. For extreme dissymmetry, i.e., axial ratios exceeding approximately 200 (which corresponds to $R_{g,z} >$ ca. 500 Å for HPMC), the calculated radii appear to be larger than those measured by light scattering despite the agreement regarding molecular weight. In other words, light scattering data on M_w and $R_{g,z}$ appear to give somewhat disparate values of α at these extreme dissymmetries. An example of the simplicity of estimating of R_g and α may be given: measurements on hydroxypropyl cellulose, HPC,[70] gave $M_w = 80,000$ and $R_g = 360$ Å, while

Table III. USP-type 2910 HPMC grade average molecular weight M_w, length l_w, radius of gyration $R_{g,w}$, the Flory radius R_F of the hydrodynamic-equivalent sphere, and radii of gyration of the Flory sphere $R_{g,F}$ and dense sphere $R_{g,s}$ calculated from viscosity of aqueous solutions at 20°C using $M_u = 203 \pm 3$ g/mol, $\rho = 1.04 \pm 0.04$ g dry polymer per mL solvated polymer,[1] $l_u = 5.15$ Å,[62] and $\alpha = 1$[1] with the following constants derived: $\mathbf{a}_u = 0.58 \pm 0.04$, $K_w = (2.8 \pm 0.2)10^{-5}$ dLg^{-1}(g/mol)$^{-1}$, $d_u = 8.9$ Å

USP Visc. grade (cP) 2% w/v, 20°C	[η] 20°C (dL/g) grade average[a]	M_n (g/mol) osmometry[b]	M_w (g/mol) calc.	M_w (g/mol) light scatt.	l_w (Å)	$R_{g,w}$ (Å) calc[c]	$R_{g,z}$ (Å) light scatt.	R_F (Å) calc.	$R_{g,F}$ (Å) calc.	$R_{g,s}$ (Å) calc.
10,000	9.4 ± 0.6	120,000	340,000	309,000[d]	8700	2500	730[d]; 1490[e] 715[f]	370	260	39
4,000	7.4 ± 0.4	100,000	270,000	225,000[d]	6800	2000	680[d]; 1260[e]	320	220	36
50	2.7 ± 0.3	31,000	98,000	132,000[d] 96,000[g]	2500	720	580[d]; 590[e] 339[g]; 251[h] 632[h]; 327[h]	160	110	26
6	0.91 ± 0.10	12,000	33,000		840	240	253[i]; 230[e]	78	55	18
3	0.65 ± 0.07	9,300	24,000		600	170	160[e]	62	44	16
unit[j]	0.00558	—	203		5.15	1.49				
unit[k]	0.0240	—	203		—	—		4.3	3.1	3.3

[a] Part II.[1]
[b] Osmometry[2]; new value for the polydispersity $P = 2.8 \pm 0.3$.
[c] l_w here equates the "contour" length L_w ($L_w = M_w l_u / M_u$) since $\alpha = 1$.
[d] Single batch HPMC in 50% methanol/50% 10 mM NaCl at 24°C.[63]
[e] Xanthan, dimeric helix of Na-salt in 0.1 M NaCl at 25°C.[67] Interpolated $R_{g,z}$ for the same DP_w as for the HPMC grade.
[f] HEC in water, DP_w ca. 2190, $[\eta] = 9.50$ dL/g at 20°C.[68]
[g] HPMC (USP-type 2906, 50 cP) in 10 mM NaCl at 30°C.[64]
[h] HPMC (USP-type 2906, 67 cP) in water and 0.5 M NaCl ($R_{g,z} = 327$ Å) at 24°C, $[\eta] = 2.85$ dL/g at 25°C.[65]
[i] CA in CH_2Cl_2/MeOH at 25°C, $DP_w = 247$, $[\eta] = 1.32$ dL/g in THF at 25°C.[69]
[j] Rod-like monomer, $[\eta]_{u,w} = \mathbf{a}_u/(100\rho)$.
[k] Spherical monomer, $[\eta]_{u,w} = 2.5/(100\ \rho)$.

Equation (16) gives $R_g = 5.15*80000/336/3.46 = 354\,Å$, assuming $M_u = 336$ and $\alpha = 1$. The agreement between calculated and measured R_g for $\alpha = 1$ strongly suggests rod shape. Actually, laminar dynamics appears to be an independent method to corroborate measurements of R_g of rod-shaped particles.

Influence of Brownian Motion

If Brownian motion could be absent it can be argued that the particle length axis should orient itself parallel to the bulk flow direction irrespective of the shear rate, as long as $D > 0$, since there would be no force counteracting orientation. However, it can be assumed that the presence of Brownian motion will cause deviation of the particle axis direction from the bulk flow direction.[1,9] This appears, nonetheless, from the equivalence of stationary $[\eta]$ and high-shear $[\eta]$, not to influence the stationary dynamics. Hence, it may be concluded that the flow direction of the liquid in the immediate vicinity of the particle must remain parallel to the particle axis independent of the Brownian motion (see assumption 10 in the prior article[1] and assumption II of this aticle's theory section). Since stationary and laminar dynamics are found to be independent of Brownian motion it follows that they also must be temperature independent. In contrast, shear-thinning dynamics is essentially dependent on, in addition to particle shape, particle orientation (see the section on critical shear rate D^* below), which is influenced by Brownian motion, and hence a dependence on temperature as well as particle dimension may then be anticipated.

Critical Shear Rate D^*

The critical shear rate D^* indicates the transition from non-Newtonian to Newtonian behavior, i.e., the borderline between dependence on and independence of Brownian motion. Hence, D^* appears to be the shear rate that balances the effect of Brownian motion. As Figure 1 illustrates D^* is independent of concentration while strongly dependent on particle shape. The combined information in Figures 1, 2, and 8 suggests that, for fully extended polymers, D^* is inversely proportional to the square of the axial ratio **a**. Interestingly enough, this proportionality also results if D^* is identified with a rotational diffusion coefficient D_r (1/s) or the inverse of a characteristic time constant θ (s), both at infinite dilution, since one may then show that

$$D^* = \frac{R\,T}{(\eta^\circ\,M\,100\,[\eta]B)} \tag{23}$$

where R is the ideal gas constant (J/mol/K), T the temperature (K), and B a dimensionless constant. Equation (23) is obtained from the Stokes-Einstein law for rotatory diffusion of a sphere[71] by scaling according to shape (proportional to $[\eta]$) and volume (proportional to M) of the particle. An experimental value $B \approx 0.1$ is obtained from the present work. Various other time constants θ have been obtained from Equation (23) (replacing D^* with $1/\theta$) for B values in the range from $B = 1.6$ to $B = 0.4$.[9,10,72]

Influence of Shear

The phenomenological effect of shear rate may physically be explained by a successive alignment of the particles' length axis with the bulk flow direction with increased shear rate, from completely unaligned at stationary conditions to fully aligned at laminar conditions occurring at shear rates exceeding a critical shear rate D^*. Hence, the shear-thinning rheology for suspensions appears to be essentially an orientation phenomenon. This description also agrees with the more general opinion[6,7,9] of a reversible structural change in the fluid, i.e., that time-independent non-Newtonian flow is due to the fact that "unbroken structure breaks down, and the fraction unbroken at zero shear is assumed to be unity."[6] Adopting this view, the characteristic time constant θ can then be regarded as a kinetic, an elastic, or a relaxation constant representative of the structural equilibrium determined by the counteracting orientational forces caused by flow and Brownian motion respectively.

Critical Concentration c* and Critical Specific Viscosity η_{sp}^*

The universal stationary dynamics, as presented in a scaled form like Figure 7, where $\log \eta_{sp}$ versus $\log c[\eta]$ has been plotted, offers the possibility of revealing the universal influence of concentration on specific viscosity. It can be seen from the broken curve calculated by Equation (6) that the slope $\delta \log \eta_{sp}/\delta \log c[\eta]$ increases monotonically and progressively, from slope = 1 to slope > 5, with increasing concentration. Hence, no particular phenomenon, like a critical concentration reflecting a change[11] in interaction mechanism, is hinted at. Nevertheless, analysis of $\log \eta_{rel}$ versus $\log c[\eta]$, using Equation (6) and k = 7.2, gives an interesting result for slope 1. At this point, Equation (24) is valid:

$$c^* = \frac{1.26}{[\eta]\ (D \to 0)} \tag{24}$$

which is deceptively close to the so called "overlap" concentration, which usually[4] is denoted by c^*, and which notation is retained here due to the

numerical similarity and since it is settled in polymer literature, introduced as "Grenzkonzentration" already by Staudinger,[73,74] who also suggested that it is caused by an onset of molecular touching. Literature estimates of c^* are essentially based on Staudinger's idea plus the concept of a particle having a much larger hydrodynamically effective volume V_h than the particle's own volume V_p. Hence, the value $c^* = 2.5/[\eta]$ is classically obtained[75] by postulating that the polymer molecule is capable of excluding a large fraction of the solvent from other polymer molecules by immobilizing or binding large quantities of solvent to the polymer molecule. In addition, it is assumed that these polymer-solvate aggregates ("coils") have more or less spherical shape so that Einstein's relation $[\eta]_\phi = 2.5$ at infinite dilution can be applied. In this way, the volume of solvated polymer per amount of dry polymer (mL/g) is calculated to be equal to $1/c^*$, as $c \to 0$, leading to the perception that all solvent is immobilized at a polymer concentration of c^*. However, such an expansion, which can be shown to be a factor $V_h/V_p = (\mathbf{a} + 1.5)/2.5 = 100[\eta]\rho/2.5$, using Einstein's relation and Equations (1) and (2), of the hydrodynamically effective volume, appears unrealistic, e.g., particles with $[\eta] = 10\,\mathrm{dL/g}$, such as HPMC 10,000 cP, would expand by a factor of approximately 400 (i.e., immobilize about 400 mL solvent per g dry particles). Other literature estimates of c^* employ the same concept and differ only in that the constant 2.5 is replaced; e.g., Fujita[4] arrives at $c^* = 1.46[\eta]$ for good solvents while Onogi et al.[76] and Cornet[77] propose that c^* can be obtained, by slope analysis of log η versus log c, as the onset of a purportedly constant slope at higher concentrations. Recalculation[43] of Cornet's data results in $c^* = 6.14/[\eta]$ for theta solvents. Generally, "overlap" is thought to occur at unit volume fraction of expanded particles ($\phi_h = 1$), corresponding to a true volume fraction of $\phi_p^* = V_p/V_h$ and a coil density $\rho_\phi^* = V_h/V_p$. The coil density can alternatively be expressed in monomers/mL coil, as preferred, for example, by de Gennes,[55,78,79] and one arrives at $\rho_m^* = 3N/(4\pi R_F^3)$ when $c \to 0$. N is the degree of polymerization and R_F (cm) is "the Flory radius, including the effects of excluded volume."[79] The expression for ρ_m^* agrees exactly with $c^* = 2.5/[\eta]$ since $4\pi R_F^3/3 = 100[\eta]\rho V_p/2.5$ when $c \to 0$.

However, the term "overlap concentration" appears misleading in view of the fact that the volume expansion postulate is not required to arrive at Equation (24). Instead, as has been argued above, the concentration dependency of viscosity may be seen as purely a matter of hydrodynamic interaction or flow perturbation (i.e., a single mechanism) without additional physical interaction, for example, in the form of touching ("overlapping"), between the particles. Hence, the concept of overlapping seems to be virtual rather than real, and c^* must be attributed to another phenomenon, if such exists at all. It is therefore of interest

that it can in fact be shown that c^*, according to Equation (24), is the concentration at which there is a maximum in the steady-state mass flow of Fickian diffusion of particles from a rate-determining diffusion layer of concentration c, if the permeability can be assumed to be proportional to $1/\eta$ into a sink with lower concentration. Therefore, c^* rather corresponds to a critical specific viscosity η^*_{sp} that determines the particle mass transport rate and as such is of importance, for example, for industrial applications of polymeric controlled-release formulations. Also, one may demonstrate, by combining Equations (6) ($k = 7.2$) and (24), that η^*_{sp} is invariable ($\eta^*_{sp} \approx 2.19$, see Figure 7) for any particle, independent of solvent or temperature. Thus, it may be concluded that η^*_{sp}, which originally was introduced as "Grenzviscosität" by Staudinger,[74] is a universal constant for all polymer suspensions/solutions.

As noted above, c^* increases with an increase in shear rate and will approach bulk particle media (i.e., unit volume fraction or 100ρg/dL) at $D > D^*$. Further, a crude measure of c^* is bestowed by the linear range, denoted by c_{lin}, of the reduced viscosity versus concentration (see Table II). However, c_{lin} is not explicitly defined and therefore largely reliant on the accuracy of the measurements; c_{lin} tends to increase with increased measurement error. Also, numerical analysis using Equation (6) proposes that both the values of c_{lin} and k_H in Table II may be overestimated.

Huggins Constant

Since the viscosity increasing effect for rod-shaped particles is weaker than for spheres per unit volume and axial ratio as concluded above, it suggests that the Huggins constant k_H is dependent on particle shape. The effect of shape is also indicated from measurements[80–82] on monodisperse polystyrene in good solvents, which show that k_H monotonically increases from $k_H \approx 0.35$ for high polymers ($[\eta] > 0.467$ dL/g in toluene at 15°C[81]) to $k_H \approx 0.83$ for spherical oligomers ($[\eta]$ approximately 0.025 dL/g in benzene at 25°C[80] or toluene at 15°C[81]). The phenomenon is even more pronounced if side chains are added to the polystyrene molecules.[83] The importance of shape is further elaborated below where the k_H for rods and spheres, under pure hydrodynamic interaction at zero shear, are estimated.

Rod-Shaped Particles

The Huggins constant can be estimated from Equation (6). The sensitivity towards the value of k is not high for this analysis, and k_H adopts a value of $k_H = 0.42$, for any $[\eta]$, in a range of k ($k = 6$ to $k = 8$) at

infinite dilution. The value of k_H agrees well with the study on polystyrenes[80,81] but is somewhat lower than the experimental findings on HPMC (the initial study[1] and the present work) and can be explained with the general tendency to overestimate k_H with increased experimental uncertainty. Since the highest precision probably was obtained for the lowest viscosity grade, i.e., HPMC 3 cP, using capillary viscometry[1] the k_H value ($k_H = 0.45$) obtained for this grade should be the most accurate. Still better accuracy might be expected for even lower $[\eta]$, although spheres should be exempted.

Unfortunately, literature[84] data on k_H for high polymers appear to be too scattered, presumably due to experimental difficulties, adsorption being one of the problems,[85–88] to reject or approve of the above value from laminar dynamics. Literature values are commonly in the range $k_H = 0.3$ to $k_H = 0.8$, and occasionally much higher, indicating particle–particle interaction or spherical shape. However, for many polymers in good solvents $k_H = 0.4 \pm 0.1$.[15] Values above 0.5 have been considered indicative of partial contribution from non-hydrodynamic interaction (e.g., particle–particle association).[89] The previously suggested[1] temperature independence of k_H has recently been supported by a study of polystyrene in a good solvent for which k_H was constant ($k_H = 0.36$) in the temperature range from –35°C to +25°C.[90]

Spherical Particles

The Huggins constant for spheres can be estimated from Equation (25):

$$\eta_{rel} = \frac{(1 + \phi/2)}{(1 - 2\phi)} \tag{25}$$

which describes the concentration dependence of the viscosity according to the treatment by Einstein.[91,92] Assuming that this relation is of the correct form at least at low concentrations one obtains a value of $k_H = 0.82$. Equation (25) is actually a very good, if not the best, approximation even up to high volume fractions (at least up to $\phi = 0.40$) as can be judged by comparison with experimental observations[93–95] of spherical particles. Previous estimates of k_H, based on the truncated Equation (25)[96] (i.e., $\eta_{sp} = 2.5\phi$, which is valid only up to ϕ approximately 0.01) or on the Gaussian random coil chain in a theta solvent,[97] arrive at $k_H = 0.76$. An experimental approach is to analyze viscosity data for solutions of nearly spherical molecules. In this way a value of $k_H = 1.1$ can be obtained from viscosity data[49] on aqueous sucrose. This value together with the close agreement with Equation (25) (up to $\phi = 0.40$ assuming $\rho = 1$ g/mL hydrated sucrose) indicates that the hydrated sucrose molecule behaves like a spherical particle.

Relation to Other Models for Suspension Hydrodynamics

The present theory seems to be in full agreement with current rheology models to which the concepts of a critical shear rate D^* and a critical specific viscosity η_{sp}^* have been added. Furthermore, good agreement with predicted and measured molecular characteristics such as molecular weight is indicated. However, although the theory referred to here as laminar dynamics agrees with general kinetic-hydrodynamic models, it distinguishes itself from some of the paradigms of prevailing[1,9,44,76,98–106] molecular-hydrodynamics. There are basically two reasons for this, namely, differences in (1) the interpretation of the Einstein relation $[\eta]_\phi = 2.5$ and (2) the perception of the transport problem. The common molecular-hydrodynamics apply the Einstein relation without modification and end up in the postulate of solvent immobilization and the idea of hydrodynamically equivalent spheres,[54,107] which results in the belief that polymers exist in the form of nearly spherical coils encapsulating a large amount of solvent. However, Fujita[108] concludes that unless the hydrodynamic mechanism for the postulate of immobilization of solvent by the polymer is clarified, the Mark-Houwink equation cannot be said to be explained by molecular theory:'' It is amazing that we are still unable to explain why actual polymer molecules behave as if non-draining for any chain length .... There must be an as yet unknown mechanism that happens to make the polymer behave as impermeable to the solvent.'' Even Flory[107] notes that "the concept of an *equivalent hydrodynamic sphere*, impenetrable to the solvent ... suffers one serious deficiency: the value of R_F remains quantitatively undefined .... A more thoroughgoing examination of the hydrodynamic interaction is needed.'' Furthermore, de Gennes[79] arrives at a divergence between observed and predicted molecular weight dependency of the viscosity and concludes,'' Thus there remains a serious problem concerning the dependence on molecular mass of the viscoelastic parameters. This may be due to some fundamental flaw in the reptation model ....'' The scaling laws in question were: $\eta_{rel} \cong (c/c^*)^{3.75}$ and $\eta \propto M^3$. The first law corresponds to $\eta_{rel} = (c[\eta]/g)^{3.75}$, since $c^* = g/[\eta]$ and where g is a constant as in Equation (24), which obviously oversimplifies the universal behavior (e.g., the scaling law is not defined at $c[\eta] < g$ as η_{rel} becomes < 1) and only approximately follows the universal behavior in a limited range of $c[\eta]$ (best fit if $g \approx 1.5$ and $2.5 < c[\eta] < 35$), as can be judged from a comparison with Equations (5) and (6) and Figure 7.

In contrast to the prevailing molecular-hydrodynamics, the present theory takes the view that the Einstein relation can be generalized to any particle shape[1] while retaining the fundamental perceptions: (1) that the viscosity increasing effect is solely due to perturbation of the flow of the dispersing fluid and (2) that the hydrodynamically effective volume of

the particle is equal to its real volume. While the prevailing molecular-hydrodynamics encompass the opinion that friction between particle and dispersing fluid as well as between or even within[109,110] particles accounts for the viscosity increase of the suspension and therefore focus on phenomena like entanglement, Brownian motion, "internal chain dynamics (hopping of individual chain "beads"),[104]" "internal viscosity,"[109,110] oscillating deformation,[111,112] "viscous drag,"[106,113] "cluster formation,"[82] etc., the standpoint taken in laminar dynamics is that the viscosity increasing effect is entirely due to friction between fluid constituents. A completely different hydrodynamic case should result if friction occurred between particle and solvent.

It appears as if the suggested laminar dynamics confer a viable alternative to predominating models on polymer hydrodynamics that is appealingly simple (being free from adjustable parameters), universal, and realistic. Furthermore, it is encouraging that the perhaps most advantageous feature of laminar dynamics, namely, its ability to estimate particle shape, is experimentally supported by recent viscometry on aqueous suspensions of particles with known shape (i.e., cellulose whiskers having $\mathbf{a} \approx 140$ and $[\eta] = 1.09\,\mathrm{dL/g}$).[114] Equations (1) and (2) give $\mathbf{a}_w = [\eta]100\rho - 1.5 = 139$ if ρ is taken to be 1.29 g dry cellulose/mL hydrated cellulose, assuming the swelling percent of the whisker to be somewhat less than its percent water content, which may be expected to be similar to microcrystalline cellulose, which takes up approximately 15%w/w of water.[115] Other important support is provided from visual and rheological observations on model fiber suspensions that confirm that, at high shear rates, the fibers align with the streamlines and that the suspension exhibits Newtonian behavior, being a function of fiber volume fraction and fiber axial ratio only.[116]

REFERENCES

[1] Lundqvist, R. (1999). Molecular weight studies on hydroxypropyl methylcellulose. II: Intrinsic viscosity. *Int. J. Polym. Anal. Charact.* **5**, 61–84.
[2] Lundqvist, R. and N. Soubbotin. (1997). Molecular weight studies on hydroxypropyl methylcellulose. I: Osmometry. *Int. J. Polym. Anal. Charact.* **4**, 173–187.
[3] Alfrey, T. (1947). The influence of solvent composition on the specific viscosities of polymer solutions. *J. Colloid. Sci.* **2**, 99–114.
[4] Fujita, H. (1990). *Polymer Solutions*. Amsterdam: Elsevier.
[5] Wilkinson, W. L. (1960). *Non-Newtonian Fluids: Fluid Mechanics, Mixing and Heat Transfer*. Oxford: Pergamon.
[6] Denny, D. A. and R. S. Brodkey. (1962). Kinetic interpretation of non-Newtonian flow. *J. Appl. Phys.* **33**, 2269–2274.

[7] Cross, M. M. (1979). Relation between viscoelasticity and shear-thinning behaviour in liquids. *Rheol. Acta* **18**, 609–614.
[8] Van Vazer, J. R., J. W. Lyons, K. Y. Kim, and R. E. Colwell. (1963). *Viscosity and Flow Measurement: A Laboratory Handbook of Rheology*. New York: Interscience-John Wiley.
[9] Vinogradov, G. V. and A. Ya. Malkin. (1980). *Rheology of Polymers: Viscoelasticity and Flow of Polymers*. Moscow: Mir Publishers, Berlin: Springer Verlag.
[10] Ferry, J. D. (1980). *Viscoelastic Properties of Polymers*, 3rd ed. New York: John Wiley.
[11] Bird, R. B., R. C. Armstrong, and O. Hassager. (1987). *Dynamics of Polymeric Liquids, Vol. 1: Fluid Mechanics*, 2nd ed. New York: John Wiley.
[12] Baker, F. S. and R. E. Carter. (1990). Industrial applications of rheology measurements. *Int. Lab.* Jan-Feb, 54–58.
[13] Park, N. A. and T. F. Irvine, Jr. (1988). Measurements of rheological fluid properties with the falling needle viscometer. *Rev. Sci. Instrum.* **59**, 2051–2058.
[14] Park, N. A. and T. F. Irvine, Jr. (1988). The falling needle viscometer: A new technique for viscosity measurements. *Am. Lab.* **20** (Nov), 57–63.
[15] Rodrigues, F. (1996). *Principles of Polymer Systems*, 4th ed., ch. 7. Washington, D.C.: Taylor and Francis, pp. 225–287.
[16] Ostwald, Wo. and R. Auerbach. (1926). Ueber die Viskosität kolloider Lösungen im Struktur-, Laminar- und Turbulenzgebiet. *Kolloid Z.* **38**, 261–280.
[17] Reiner, M. and R. Schoenfeld-Reiner. (1933). Viskosimetrische Untersuchungen an Lösungen hochmolecularen Naturstoffe. I. Mitteilung. Kautschuk in Toluol. *Kolloid Z.* **65**, 44–62.
[18] Reiner, M. (1934). Viscometric studies of rubber solutions. *Physics* **5**, 342–349.
[19] Philippoff, W. and K. Hess. (1936). Zum Viscositätsproblem bei organischen Kolloiden. *Z. Physik. Chem.* **B3**, 237–255.
[20] Philippoff, W. (1936). Die Bedeutung der Viskosität für die Chemie der Cellulose. *Die Cellulosechemie.* **17**, 57–77.
[21] Timell, T. E. (1954). The effect of rate of shear on the viscosity of dilute solutions of cellulose nitrate. *Sven. Papperstidn.* **57**, 777–788.
[22] Brodnyan, J. G., F. H. Gaskin, W. Philippoff, and E. G. Lendrat. (1958). The rheology of various solutions of cellulose derivatives. *Trans. Soc. Rheol.* **2**, 285–302.
[23] Brodnyan, J. G., F. H. Gaskin, and W. Philippoff. (1957). On normal stresses, flow curves, flow birefingence, and normal stresses of polyisobutylene solutions. Part II: Experimental. *Trans. Soc. Rheol.* **1**, 109–118.
[24] Merrill, E. W. (1959). Intrinsic viscosity by high shear determination: Polyisobutylene solutions. *J. Polym. Sci.* **38**, 539–543.
[25] Merrill, E. W., H. S. Mickley, A. Ram, and G. Perkinson. (1961). Upper Newtonian regime in polymer solutions. I: Polystyrenes in toluene. *Trans. Soc. Rheol.* **5**, 237–246.

[26] Yang, J. T. (1958). Non-Newtonian viscosity of poly-γ-benzyl-L-glutamate solutions. *J. Am. Chem. Soc.* **80**, 1783–1788.
[27] Yang, J. T. (1959). Factors affecting the non-Newtonian viscosity of rigid particles. *J. Am. Chem. Soc.* **81**, 3902–3907.
[28] De Waele, A. (1923). Viscometry and plastometry. *J. Oil Colour Chem. Assoc.* **6**, 33–69.
[29] Ostwald, Wo. (1925). Ueber die Geschwindigkeitsfunktion der Viskosität disperser Systeme. I. *Kolloid Z.* **36**, 99–114.
[30] Yasuda, K., R. C. Armstrong, and R. E. Cohen. (1981). Shear flow properties of concentrated solutions of linear and star branched polystyrenes. *Rheol. Acta* **20**, 163–178.
[31] Middleman, S. (1968). *The Flow of High Polymers: Continuum and Molecular Rheology.* New York: Interscience, p. 28.
[32] Berry, D. H. and W. B. Russel. (1987). The rheology of dilute suspensions of slender rods in weak flows. *J. Fluid Mech.* **180**, 475–494.
[33] Chauveteau, G. (1982). Rodlike polymer solution flow through fine pores: Influence of pore size on the rheological behaviour. *J. Rheol.* **26**, 111–142.
[34] Tsenoglou, C. (2001). Non-Newtonian rheology of entangled polymer solutions and melts. *Macromolecules* **34**, 2148–2155.
[35] Baker, F. (1913). The viscosity of cellulose nitrate solutions. *J. Chem. Soc.* **103**, 1653–1675.
[36] Onogi, S., S. Kimura, T. Kato, T. Masuda, and N. Miyanaga. (1966). Effects of molecular weight and concentration on flow properties of concentrated polymer solutions. *J. Polym. Sci. C* **15**, 381–406.
[37] Onogi, S., T. Masuda, N. Miynaga, and Y. Kimura. (1967). Dependence of viscosity of concentrated polymer solutions upon molecular weight and concentration. *J. Polym. Sci. Part A-2* **5**, 899–913.
[38] Johnson, M. F., W. W. Evans, I. Jordan, and J. D. Ferry. (1952). Viscosities of concentrated polymer solutions. II: Polyisobutylene. *J. Colloid Sci.* **7**, 498–510.
[39] Takada, Y., T. Sato, and A. Teramoto. (1991). Dynamics of stiff-chain polymers in isotropic solution. 2: Viscosity of aqueous solutions of xanthan, a rigid double-helical polysaccaride. *Macromolecules* **24**, 6215–6219.
[40] Ohshima, A., H. Kudo, T. Sato, and A. Teramoto. (1995). Entanglement effects in semiflexible polymer solutions. 1: Zero-shear viscosity of poly(n-hexyl isocyanate) solutions. *Macromolecules* **28**, 6095–6099.
[41] Ohshima, A., A. Yamagata, T. Sato, and A. Teramoto. (1999). Entanglement effects in semiflexible polymer solutions. 3: Zero-shear viscosity and mutual diffusion coefficient of poly(n-hexyl isocyanate) solutions. *Macromolecules* **32**, 8645–8655.
[42] Graessley, W. W., R. L. Hazleton, and L. R. Lindeman. (1967). The shear-rate dependence of viscosity in concentrated solutions of narrow-distribution polystyrenes. *Trans. Soc. Rheol.* **11**, 267–285.
[43] Graessley, W. W. (1974). The entanglement concept in polymer rheology. *Adv. Polym. Sci.* **16**.
[44] Doi, M. and S. F. Edwards. (1986). *The Theory of Polymer Dynamics*. Oxford: Clarendon.

[45] Rodriguez, F. and L. A. Goettler. (1964). The flow of moderately concentrated polymer solutions in water. *Trans. Soc. Rheol.* **8**, 3–17.
[46] Abdel-Alim, A. H., S. T. Balke, and A. E. Hamielec. (1973). Flow properties of polystyrene solutions under high shear rates. *J. Appl. Polym. Sci.* **17**, 1431–1442.
[47] Mardles, E. W. J. (1923). The viscosity of some cellulose acetate solutions. *J. Chem. Soc.* **123**, 1951–1957.
[48] Sakurada, I. (1933). Einfluss der Teilchenform und des spezifischen Volumens auf die Viskosität lyophiler Kolloide. *Kolloid Z.* **64**, 195–200.
[49] *Handbook of Chemistry and Physics*. (1976–1977). 57th ed. D-261. Cleveland: Chemical Rubber Publishing Company.
[50] Aharoni, S. M. (1977). On the relationship between K and *a* and between K_θ and the molecular weight per chain atom. *J. Appl. Polym. Sci.* **21**, 1323–1339.
[51] Errata: Equations (21) and (22) in [1] should read

$$\psi^{3/2} = \mathrm{M_w}\mathbf{a}_\mathrm{u}/(\mathrm{M_u}\mathbf{a}_\mathrm{w}\mathbf{a}_\mathrm{l}) = \mathrm{M_w}\mathbf{a}_\mathrm{u}/(\mathrm{M_u}([\eta]100\rho - 1.5)\mathbf{a}_\mathrm{l}) \qquad (21)$$

$$1_\mathrm{w}^3 = \psi^{3/2}(\mathbf{a}_\mathrm{w}\mathbf{a}_\mathrm{l}1_\mathrm{u}/\mathbf{a}_\mathrm{u})^3 = \mathrm{M_w}([\eta]100\rho - 1.5)^2\mathbf{a}_\mathrm{l}^2 1_\mathrm{u}^3/(\mathrm{M_u}\mathbf{a}_\mathrm{u}^2) \qquad (22)$$

[52] Flory, P. J. (1961). Phase changes in proteins and polypeptides. *J. Polym. Sci.* **49**, 105–128.
[53] Tanford, C. (1961). *Physical Chemistry of Macromolecules*. New York: Wiley, p. 306.
[54] Flory, P. J. (1949). The configuration of real polymer chains. *J. Chem. Phys.* **17**, 304–310.
[55] De Gennes, P. G. (1979). *Scaling Concepts in Polymer Physics*. Ithaca, N.Y.: Cornell University Press.
[56] Staudinger, H. and H. Freudenberger. (1930). Über hochpolymere Verbindungen, 41. Mitteilung: Molekulargewichts-Bestimmungen an Acetylcellulosen. *Ber. Deutsch. Chem. Ges.* **63**, 2331–2343.
[57] Eisenschitz, R. (1931). Die Viscosität von Suspensionen langgestreckter Teilchen und ihre Interpretation durch Raumbeanspruchung. *Z. Physik. Chem.* **A158**, 78–90.
[58] Kuhn, W. (1932). Dehnungsdoppelbrechung von Kolloiden in Lösung. *Z. Physik. Chem.* **A161**, 427–440.
[59] Kuhn, W. (1933). Über quantitative Deutung der Viskosität und Strömungsdoppelbrechung von Suspensionen. *Kolloid Z.* **62**, 269–285.
[60] Kuhn, W. (1934). Über die Gestalt fadenförmiger Molecüle in Lösungen. *Kolloid Z.* **68**, 2–15.
[61] Kuhn, W. (1936). Gestalt und Eigenschaften fadenförmiger Molecüle in Lösungen (und im elastisch festen Zustande). *Z. Angew. Chem.* **49**, 858–862.
[62] Kiessig, H. (1950). Die Beeinflussung der Kristallgitter von Zellulose I und Zellulose II dursch Wasser. Die Bestimmung der Gitterzellen, der röntgenographischen Dichten und der Einfluss von Wasser auf die Gitterzellen. *Z. Electrochem. Angew. Physik. Chem.* **54**, 320–325.
[63] Wittgren, B. and K.-G. Wahlund. (1997). Effects of flow-rates and sample concentration on the molar mass characterisation of modified celluloses

using assymetrical flow field-flow fractionation-multi-angle light scattering. *J. Chromatogr. A* **791**, 135–149.

[64] Poché, D. S., A. L. Ribes, and D. L. Tipton. (1998). Characterization of Methocel™: Correlation of static light-scattering data to GPC molar mass data based on pullulan standards. *J. Appl. Polym. Sci.* **70**, 2197–2210.

[65] Neely, W. B. (1963). Solution properties of polysaccarides. IV: Molecular weight and aggregate formation in methylcellulose solutions. *J. Polym. Sci.* **A1**, 311–320.

[66] Nilsson, S., L.-O. Sundelöf, and B. Porsch. (1995). On the characterization principles of some technically important water soluble non-ionic cellulose derivatives. *Carbohydr. Polym.* **28**, 265–275.

[67] Sato, T., T. Norisuye, and H. Fujita. (1984). Double-stranded helix of xanthan: Dimensional and hydrodynamic properties in 0.1 M aqueous sodium chloride. *Macromolecules* **17**, 2696–2700.

[68] Brown, W. (1961). Hydroxyethyl cellulose: A study of its macromolecular properties in solution. *Arkiv kemi* **18**, 227–284.

[69] Tanner, D. W. and G. C. Berry. (1974). Properties of cellulose acetate in solution. I: Light scattering, osmometry, and viscometry on dilute solutions. *J. Polym. Sci. Polym. Phys. Ed.* **12**, 941–975.

[70] Gao, J., G. Haidar, X. Lu, and Z. Hu. (2001). Self-association of hydroxypropylcellulose in water. *Macromolecules* **34**, 2242–2247.

[71] Brenner, H. (1967). Coupling between translational and rotational Brownian motions of rigid particles of arbitrary shape. II: General theory. *J. Colloid Interface Sci.* **23**, 407–436.

[72] Bird, R. B., C. F. Curtiss, R. C. Armstrong, and O. Hassager. (1987). *Dynamics of Polymeric Liquids, Vol. 2: Kinetic Theory*, 2nd ed. New York: John Wiley, p. 123.

[73] Staudinger, H. (1930). Über Isopren und Kautschuk, 20. Mitteil.: Über die Kolloidnatur von Kautschuk, Guttapercha und Balata. *Ber. Deutsch. Chem. Ges.* **63**, 921–934.

[74] Staudinger, H. (1932). *Die hochmolekularen organischen Verbindungen – Kautschuk und Cellulose*. Berlin: Springer.

[75] Vollmert, B. (1962). *Grundriss der makromolekularen Chemie.* Berlin: Springer, pp. 348–385.

[76] Onogi, S., T. Kobayashi, Y. Kojima, and Y. Tanigushi. (1963). Non-Newtonian flow of concentrated solutions of high polymers. *J. Appl. Polym. Sci.* **7**, 847–859.

[77] Cornet, C. F. (1965). The determination of unperturbed dimensions of polymer molecules by viscometry of moderately concentrated solutions. *Polymer* **6**, 373–384.

[78] De Gennes, P. G. (1976). Dynamics of entangled polymer solutions. I: The Rouse model. *Macromolecules* **7**, 587–593.

[79] De Gennes, P. G. (1976). Dynamics of entangled polymer solutions. II: Inclusion of hydrodynamic interactions. *Macromolecules* **7**, 594–598.

[80] Einaga, Y., H. Koyama, T. Konishi, and H. Yamakawa. (1989). Intrinsic viscosity of oligo- and polystyrenes. *Macromolecules* **22**, 3419–3424.

[81] Abe, F., Y. Einaga, and H. Yamakawa. (1993). Excluded-volume effects on the intrinsic viscosity of oligomers and polymers of styrene and isobutylene. *Macromolecules* **26**, 1891–1897.
[82] Pan, Y. and R.-S. Cheng. (2000). A novel interpretation of concentration dependence of viscosity of dilute polymer solutions. *Chin. J. Polym. Sci.* **18**, 57–67.
[83] Terao, K., T. Hokajo, Y. Nakamura, and T. Norisuye. (1999). Solution properties of polymacromonomers consisting of polystyrene. 3: Viscosity behavior in cyclohexane and toluene. *Macromolecules* **32**, 3690–3694.
[84] Stickler, M. and N. Sütterlin. (1989). Concentration dependence of the viscosity of dilute polymer solutions: Huggins and Schulz-Blaschke coefficients. In *Polymer Handbook*, eds. J. Brandrup and E. H. Immergut, 3rd ed. New York: Wiley Interscience, pp. VII/183–VII/203.
[85] Öhrn, O. E. (1958). Precision viscometry of extremely dilute solutions of high polymers. *Arkiv kemi* **12**, 397–436.
[86] Cheng, R., Y. Shao, M. Liu, and R. Qian. (1998). Effect of adsorption on the viscosity of dilute polymer solution. *Eur. Polym. J.* **34**, 1613–1619.
[87] Cheng, R., Y. Yang, and X. Yan. (1999). The wall effect on the viscosity measurement of dilute aqueous solutions of polyethylene glycol and polyvinyl alcohol using a paraffin-coated capillary viscometer. *Polymer* **40**, 3773–3779.
[88] Bercea, M., S. Morariu, C. Ioan, S. Ioan, and B. C. Simionescu. (1999). Viscometric study of extremely dilute polyacrylonitrile solutions. *Eur. Polym. J.* **35**, 2019–2024.
[89] Lewandowska, K., D. U. Staszewska, and M. Bohdanecky. (2001). The Huggins viscosity coefficient of aqueous solutions of poly(vinyl alcohol). *Eur. Polym. J.* **37**, 25–32.
[90] Osaki, K., T. Inoue, and T. Uematsu. (2000). Viscoelastic properties of dilute polymer solutions: The effect of varying the concentration. *J. Polym. Sci., Part B: Polym. Phys.* **39**, 211–217.
[91] Einstein, A. (1906). Eine neue Bestimmung der Molecüldimensionen. *Ann. Phys.* **19**, 289–306.
[92] Einstein, A. (1911). Berichtigung zu meiner Arbeit: "Eine neue Bestimmung der Molecüldimensionen." *Ann. Phys.* **34**, 591–592.
[93] Rutgers, Ir. R. (1962). Relative viscosity and concentration. *Rheol. Acta* **2**, 305–348.
[94] Thomas, D. G. (1965). Transport characteristics of suspension. VIII: A note on the viscosity of Newtonian suspensions of uniform spherical particles. *J. Colloid Sci.* **20**, 267–277.
[95] de Kruif, C. G., E. M. F. van Iersel, A. Vrij, and W. B. Russel. (1985). Hard sphere colloidal dispersions: Viscosity as a function of shear rate and volume fraction. *J. Chem. Phys.* **83**, 4717–4725.
[96] Brinkman, H. C. (1952). The viscosity of concentrated suspensions and solutions. *J. Chem. Phys.* **20**, 571.
[97] Freed, K. F. and S. F. Edwards. (1975). Huggins coefficient for the viscosity of polymer solutions. *J. Chem. Phys.* **62**, 4032–4035.

[98] He, S. and H. A. Scheraga. (1998). Macromolecular conformational dynamics in torsional angle space. *J. Chem. Phys.* **108**, 271–286.
[99] Agarwal, U. S., R. Bhargava, and R. A. Mashelkar. (1998). Brownian dynamics simulation of a polymer molecule in solution under elongational flow. *J. Chem. Phys.* **108**, 1610–1617.
[100] Andrews, N. C., A. J. McHugh, and J. D. Schieber. (1998). Conformational and rheological dynamics of semiflexible macromolecules undergoing shear flow: A nonequilibrium Brownian dynamics study. *J. Rheol.* **42**, 281–305.
[101] Prakash, J. R. and H. C. Öttinger. (1999). Viscometric functions for a dilute solution of polymers in a good solvent. *Macromolecules* **32**, 2028–2043.
[102] Volkov, V. S. and A. I. Leonov. (1999). Linear viscoelasticity of dilute polymer solutions in a viscoelastic solvent. *Macromolecules* **32**, 7666–7673.
[103] Liao, Q., L. Chen, X. Qu, and X. Jin. (2000). Brownian dynamics simulation of film formation of mixed polymer latex in the water evaporation stage. *J. Colloid Interface Sci.* **227**, 84–94.
[104] Edwards, S. F. and K. F. Freed. (1974). Theory of the dynamical viscosity of polymer solutions. *J. Chem. Phys.* **61**, 1189–1202.
[105] Yamakawa, H. (1999). A new framework for polymer solution science: The helical wormlike chain. *Polymer J.* **31**, 109–119.
[106] Mhetar, V. R. and L. A. Archer. (2000). A new proposal for polymer dynamics in steady shearing flows. *J. Polym. Sci. Part B: Polym. Phys.* **38**, 222–233.
[107] Flory, P. G. (1953). *Principles of Polymer chemistry*. Ithaca, N.Y.: Cornell University Press, p. 606.
[108] Fujita, H. (1990). *Polymer Solutions*. Amsterdam: Elsevier, p. 53.
[109] Kuhn, W. and H. Kuhn. (1945). Bedeutung beschränkt freier Drehbarkeit für die Viskosität und Strömmungsdoppelbrechung von Fadenmolekellösungen. I. *Helv. Chim. Acta* **28**, 1533–1579.
[110] Kuhn, W. and H. Kuhn. (1946). Bedeutung beschränkt freier Drehbarkeit für die Viskosität und Strömmungsdoppelbrechung von Fadenmolekellösungen. II. *Helv. Chim. Acta* **29**, 71–94.
[111] Peterlin, A. (1952). Effect of the velocity gradient on the intrinsic viscosity of polymers in solution. *J. Polym. Sci.* **8**, 621–632.
[112] Peterlin, A. (1960). Gradient dependence of intrinsic viscosity of freely flexible linear macromolecules. *J. Chem. Phys.* **33**, 1799–1802.
[113] Hassager, O. (1974). Kinetic theory and rheology of bead-rod models for macromolecular solutions. I: Equilibrium and steady flow. *J. Chem. Phys.* **60**, 2111–2124.
[114] Bercea, M. and P. Navard. (2000). Shear dynamics of aqueous suspensions of cellulose whiskers. *Macromolecules* **33**, 6011–6016.
[115] Amidon, G. E. and M. E. Houghton. (1995). The effect of moisture on the mechanical and powder flow properties of microcrystalline cellulose. *Pharm. Res.* **12**, 923–929.
[116] Mongruel, A. and M. Cloitre. (1999). Shear viscosity of suspensions of aligned non-Brownian fibres. *Rheol. Acta* **38**, 451–457.